Journal of Theoretical and Applied Mechanics, Sofia, Vol.52 (2022) pp. 232-247
INTERDISCIPLINARY TOPICS

SIMULATION OF ATMOSPHERIC TRANSPORT OF POLLUTANTS FROM MICRO- TO CITY-SCALE USING CFD MODEL AND UNSTRUCTURED GRIDS

ALEXANDER KHALCHENKOV[1,2], IVAN V. KOVALETS[1*]

[1]*Institute of Mathematical Machines & Systems Problems NAS of Ukraine, prosp. Glushkova, 42, 03187, Kyiv, Ukraine*
[2]*Ukrainian Center of Environmental and Water Projects, prosp. Glushkova, 42, 03187, Kyiv, Ukraine*

[Received: 20 July 2021. Accepted: 05 April 2022]

doi: https://doi.org/10.55787/jtams.22.52.3.232

ABSTRACT: The OpenFoam CFD code was adapted to simulate atmospheric transport of pollutants. By performing calculations on unstructured grids and using the modifications of turbulence parameterizations to account for the influence of Earth's rotation on PBL structure, the presented model can take into account the influence of urban obstructions and complex topography on atmospheric dispersion from a city to street-scale. The normalized mean squared error of simulated results for the conditions of the known MUST experiment was comparable with the results of other models (NMSE ≈ 0.6). The value of turbulent Schmidt number in this experiment was estimated to be Sc ≈ 0.4. The example of model application for the assessment of atmospheric pollution created by the industrial site of uranium production was presented.

KEY WORDS: OpenFoam, unstructured grids, atmospheric transport, urban, pollution, MUST experiment.

1 INTRODUCTION

Presently computational fluid dynamics (CFD) codes are widely used for assessments of the near-field (street- or micro-scale) atmospheric dispersion of pollutants in different air pollution studies [1–4]. When applied in urban air pollution studies such models are capable to account for the influence on atmospheric transport of the circulations created by interactions of buildings and other obstacles with airflow. At the same time calculation of the atmospheric transport at larger scales (city-scale) on obstacles-resolving grids with using such models remains a difficult task because of heavy computational requirements. This problem could be partially solved by the

*Corresponding author e-mail: ivkov084@gmail.com

application of the unstructured grids as in [2] which allows for increasing spatial resolution in the areas of special interest while making resolution coarser in other parts of the computational domain. Also, when considering atmospheric transport at larger scales the influence of the Earth's rotation on planetary boundary layer (PBL) structure and finally on turbulence and pollutants' mixing in the atmosphere have to be accounted for. This problem is usually solved by coupling CFD models with mesoscale meteorological models, as in [3]. Such coupling is usually implemented by imposing boundary conditions in CFD models using meteorological variables, calculated by mesoscale meteorological models. However, most of the existing CFD codes also require certain modifications in governing equations to account for the influence of Earths' rotation on turbulent atmospheric transport.

OpenFoam [5] is the famous CFD code that was used in previous studies for the calculation of atmospheric pollutants' transports, for example in [6]. Therefore, the goal of the present paper is to include in OpenFoam the parameterization of the influence of the Earth's rotation on turbulence in atmospheric PBL and to combine it with the state-of-art methods of unstructured grids generation for calculations of the atmospheric dispersion of air pollutants from micro- to city-scale in presence of complex urban obstructions and underlying topography. In the forthcoming chapters, the developed method is presented and validated against field experiment on PBL structure and laboratory experiment on atmospheric transport in urban obstructed geometries. Finally, the application of the method to the real-case problem of assessment of atmospheric pollution created by the contaminated building of the former uranium production facilities is demonstrated.

2 Basic Equations

The wind velocity field is determined by solving the stationary equations of the hydrodynamics of an incompressible fluid, averaged by Reynolds, without taking into account the processes of heat transfer [7]. The continuity and the momentum conservation equations have the form:

$$\nabla \cdot \vec{U} = 0\,, \tag{1}$$

$$\vec{U} \cdot \nabla \vec{U} - \nabla \cdot (\nu_T \nabla \vec{U}) = -[\vec{f} \times (\vec{U} - \vec{U}_g)] - \nabla p\,, \tag{2}$$

where $\vec{U} = (u_1, u_2, u_3)$ is the velocity vector, ν_T is the kinematic turbulent viscosity obtained from the turbulence parameterization presented below. Equations (1) and (2) describe the influence of the Coriolis force on the processes in the atmospheric boundary layer. In equation (2) $\bar{f} = (0, 0, f)$ is the Coriolis vector, $f = 2\Omega \sin(\varphi)$, Ω is the angular velocity of the Earth rotation, φ is latitude, $\bar{U}_g$ is the wind velocity

vector at the upper boundary of the boundary layer that is taken equal to the corresponding value of the geostrophic wind [8].

The coefficient of turbulent viscosity is parameterized by using the known relation which describes the dependence of this flow parameter on the kinetic energy of turbulent pulsations k and the rate of dissipation of the turbulent kinetic energy ε [9]:

$$\nu_T = C_\mu \frac{k^2}{\varepsilon}\,. \tag{3}$$

To calculate the kinetic energy of turbulence, the standard equation is used [9]:

$$u_j \frac{\partial k}{\partial x_j} = -\tau_{ij}\frac{\partial u_i}{\partial x_j} - \varepsilon + \frac{\partial}{\partial x_j}\Big[(\nu + \nu_t)\frac{\partial k}{\partial x_j}\Big]. \tag{4}$$

The stress tensor is calculated as for the case of an incompressible fluid [7]:

$$\tau_{ij} = -\nu_T\Big(\frac{\partial u_i}{\partial x_j} + \frac{\partial u_j}{\partial x_i}\Big) + \frac{2}{3}\delta_{ij}k\,. \tag{5}$$

Two alternative approaches are used to calculate the dissipation rate. In the first approach (one parameter turbulence model) the known relationship $\varepsilon = C_\mu^{3/4}k^{3/2}/l$ for dissipation rate is utilized which states that ε is inversely proportional to the dominating length-scale l of turbulent disturbances [9]. According to [10] this length scale could be parameterized as: $1/l = (1/k\cdot d + 1/l_h)$, where $k = 0.41$ is the von Kármán constant, d is the minimum distance to the solid boundary, l_k is the geostrophic scale of mixing, which accounts for the limited depth of the atmospheric PBL. Then the value of ε is calculated explicitly using an algebraic relation:

$$\varepsilon = C_\mu^{3/4}k^{3/2}\Big(\frac{1}{kd} + \frac{1}{l_h}\Big). \tag{6}$$

According to [10] the value for l_k is assigned to:

$$l_h = C_h U_g/f\,. \tag{7}$$

The constant $C_h = 0.00023$ was selected to best match the simulation results with the data of the "Leipzig profile" as shown below and was quite close to the corresponding value known from the literature $C_h = 0.00027$ [10]. In the second approach (modified $k-\varepsilon$ model), it is necessary to solve the equation for dissipation rate ε:

$$u_j\frac{\partial \varepsilon}{\partial x_j} = -C_{\varepsilon 1}^{*}\frac{\varepsilon}{k}\tau_{ij}\frac{\partial u_i}{\partial x_j} - C_{\varepsilon 2}\frac{\varepsilon^2}{k} + \frac{\partial}{\partial x_j}\Big[\Big(\nu + \frac{\nu_t}{\sigma_\varepsilon}\Big)\frac{\partial \varepsilon}{\partial x_j}\Big] \tag{8}$$

with the standard values of constants: $C_\mu = 0.09$, $C_{\varepsilon 2} = 1.92$, $\sigma_\varepsilon = 1.3$ [9].

The influence of the Earth's rotation on the dissipation energy is carried out according to [11] by adjusting the value of the parameter $C^*_{\varepsilon 1}$. Unlike the standard $k-\varepsilon$ model it is not a constant but depends on the ratio of the two length scales: the local scale of turbulent mixing $l_t = C_\mu^{3/4} k^{3/2}/\varepsilon$ and the geostrophic scale of mixing l_h (7). At each time step, the values of the local mixing scale l_t and $C^*_{\varepsilon 1}$ are calculated for each cell:

$$C^*_{\varepsilon 1} = C_{\varepsilon 1} + (C_{\varepsilon 2} - C_{\varepsilon 1}) \frac{l_t}{l_h} \,. \tag{9}$$

Here the value of the constant $C_{\varepsilon 1} = 1.44$ is standard for the $k-\varepsilon$ turbulence model [9].

The calculation of pollution transfer in the case of a stationary source was carried out by solving the stationary transfer equation taking into account the processes of turbulent mixing:

$$\nabla \cdot (\vec{U} C) - \Delta \left((D_0 + \nu_c)\, C \right) - q_s = 0 \,, \tag{10}$$

where q_s is the volume density of sources, C is concentration, $D_0 = 1.2 \times 10^{-5}$ m^2/s is the molecular diffusion coefficient, ν_c is the turbulent diffusion coefficient, $\nu_c = \nu_T/\mathrm{Sc}$. Here Sc is the turbulent Schmidt number. Its value in turbulent flow in urban conditions could be within the range from 0.2 to 1.3 [12].

For the numerical solutions in the OpenFoam, we used the second-order TVD numerical scheme with the OSPRE limiter for the approximation of divergence [5].

3 Construction of an Unstructured Computational Grid

The ability to use unstructured mesh allows refining a mesh in the necessary places instead of the use of the refined mesh in the entire computational domain. When modeling the atmospheric processes, it is convenient to use a computational grid that is unstructured only in the horizontal direction and structured in the vertical direction. Construction of an unstructured grid consists of the two main stages:

- construction of geometry – large-scale three-dimensional modeling of the entire area of calculations with the appointment of characteristic properties of individual geometric objects: points, lines, faces, volumes;
- construction of the calculation grid – the procedure of triangulation in accordance with the geometry, taking into account the properties of geometric objects. That is, filling the calculation area with finite volumes and assigning the types of boundary conditions for the faces bounding the calculation area.

Both steps could be performed using the GMSH program [13], designed to create three-dimensional computational grids. The advantages of this program, that is freely available on the Internet, are: 1) the availability of its own tools for constructing large-scale geometry; 2) the ability to set boundary conditions for geometric faces, and 3) its own tools for constructing a grid of finite elements according to geometry. An additional advantage of using this program is the presence in the standard package of OpenFoam of the utility gmshToFoam, which allows for converting the original format of the GMSH program directly into the OpenFoam data set.

However, the GMSH program does not have its own tools that allow for linking the computational grid to the coordinates and to take into account the topography and land-use of the underlying surface. There is a need to solve three additional subtasks: 1) binding of a three-dimensional computational grid to geographical coordinates; 2) taking into account the topography, and 3) determination of the roughness parameter. The algorithm for the solution of those tasks was developed in [14]. In the GMSH program, we first create a two-dimensional computational grid referenced to geographic coordinates using the UTM coordinate system. The use of an unstructured mesh allows for refining of a coarse mesh in the required places of the computational domain (Fig. 1). Further, by extruding the outlines of the buildings, we get a three-dimensional mesh consisting of horizontal layers. For each external face in the GMSH program, we indicate the type of the boundary condition.

Global data set such as SRTM is used to take into account the topography characteristics of the underlying surface. The topography is taken into account according to the approach described in [14], by shifting nodes according to topographic data and further smoothing the grid. This approach makes it possible to obtain a three-dimensional mesh structured vertically and unstructured horizontally. The created mesh has a flat and horizontal upper boundary and horizontal layers of cells adjacent to roofs. A lower boundary has a complex shape that reproduces the topography of the underlying surface.

For correct reproduction of wind profiles near solid surfaces without modeling of a turbulent layer on a very detailed grid, the OpenFoam program implements wall functions. The most widely used wall function in solving atmospheric problems for turbulent viscosity is the function that provides the correct logarithmic velocity profile and depends on the value of the roughness parameter (nutkAtmRoughWallFunction option in OpenFoam). The spatial distribution of the roughness parameter for the lower boundary of the computational domain can be obtained from the global datasets of land use categories, such as Modis and Globeland30. The procedure for assigning the obtained roughness fields to the corresponding faces of the OpenFoam computational grid is also described in [14].

Fig. 1: Example of two-dimensional unstructured mesh with the refined mesh in the area of the Pridneprovsky Chemical Plant (described in section 4.3).

4 Results of Calculations

4.1 Verification of the model using field experiment on PBL structure

The creation of the theory of the atmospheric PBL was associated with difficulties in obtaining field experimental data adequate to test the theory. One of classical data sets on which the theory of the atmospheric PBL could be tested is the field experiment on PBL structure [15], also known as "Leipzig profile". This experiment allows verifying the corrections introduced into the model to take into account the influence of Earths' rotation on the characteristics of the atmospheric boundary layer.

When modeling the experiment [15], the atmosphere was assumed to be inhomogeneous only in the vertical direction, the stratification was assumed neutral. The modeling parameters were set as follows: Coriolis parameter $f = 0.00014$ 1/s; geostrophic wind was directed along x-axis and had magnitude: $Ug = 17.5$ m/s; roughness parameter $z_0 = 0.3$ m; air density $\rho = 1.25$ kg/m^3. The simulation was performed for the horizontally homogeneous conditions, but a three-dimensional problem was solved. The area of calculations was limited by the following boundary conditions. At all lateral boundaries for all variables, zero gradients along normals to the boundary surfaces were assumed: $\frac{\partial}{\partial n}\phi = 0$.

At the upper boundary – fixed values were set for wind velocity components: (Ug, 0, 0) and zero gradients for other variables were assumed. At the lower solid boundary wall functions were used to simulate the logarithmic boundary layer. The following specific options according to OpenFoam documentation were used [5]: epsilonWallFunction for dissipation rate, kqRWallFunction for turbulent kinetic energy, nutkAtmRoughWallFunction for turbulent viscosity, fixed zero value for wind velocity, and zeroGradient for pressure. For the initial conditions, a fixed value of 1e-14 was assumed for all variables, since it is assumed that the result of solving the stationary problem does not depend on the initial conditions.

As it is known from other works [16] and confirmed in this work, the standard k–ε model of turbulence poorly reproduces the profile in the atmospheric PBL, especially for turbulent viscosity. The results of using a one-parameter model of turbulence with a characteristic geostrophic scale and a modified $k-\varepsilon$ model of turbulence with a variable coefficient are much better but significantly depend on the selected value of the geostrophic scale (Figs. 2 and 3). Both modified turbulence models reproduced the Leipzig profile much better than the unchanged standard $k-\varepsilon$ turbulence model.

Note that the best results of each of the models are achieved at slightly different values of the geostrophic scale. For a one-parameter model, the corresponding value is $l_h = 35$ m, while for a modified k–ε model, the corresponding value is $l_h = 30$ m.

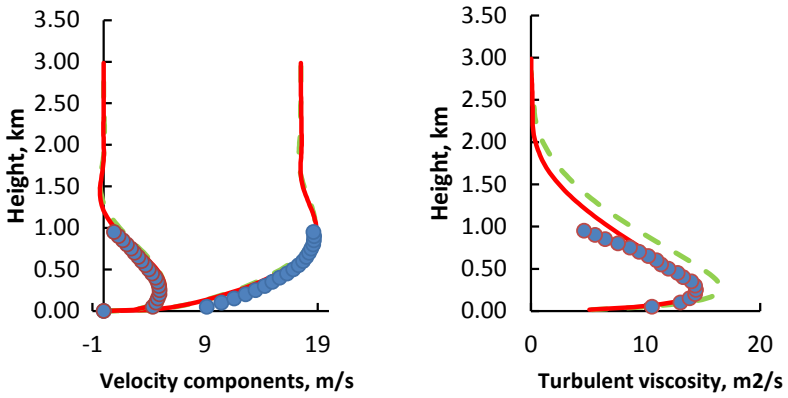

(A) (B)

Fig. 2: Measured and simulated with a modified one-parameter model of turbulence vertical profiles of meteorological variables for the conditions of experiment [15]; (A) x- and y-velocity components; (B) turbulent viscosity; points – measurements, adapted from [16]; lines – simulation results with $l_h = 40$ m (dashed line) and $l_h = 35$ m (solid line).

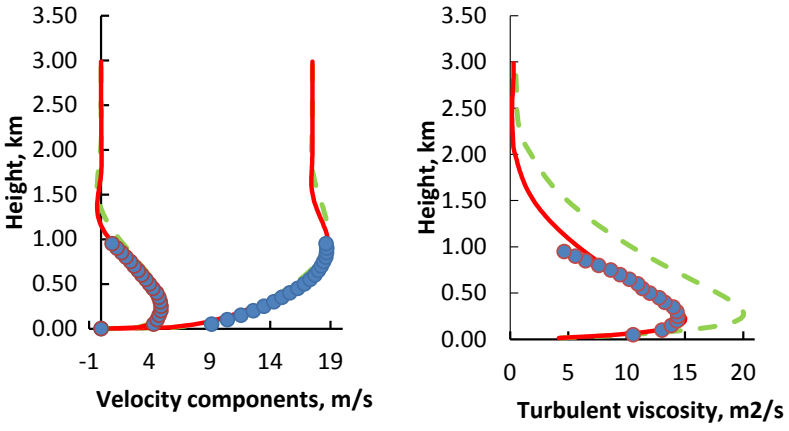

(A) (B)

Fig. 3: Measured and simulated with a modified $k-\varepsilon$ turbulence model vertical profiles of meteorological variables for the conditions of experiment [15]; (A) x- and y-velocity components; B) turbulent viscosity; points – measurements, adapted from [16]; lines – simulation results with $l_h = 40$ m (dashed line) and $l_h = 30$ m (solid line).

4.2 Verification of the model using data of MUST experiment

The ability of model to reproduce microscale features of atmospheric transport in presence of urban obstructions was verified for the conditions of the "Mock Urban Setting Test – MUST" experiment which was conducted in 2001 on a US military test site. In this field experiment, the distribution of pollution from the ground-level source in urban obstructed geometries was studied. At the experimental test site, 120 containers were installed, having dimensions: 12.2 m length, 2.54 m height, and 2.42 m width, which represented urban obstructions. Containers were placed in 10 rows with 12 containers in each row (Fig. 4). To verify OpenFoam, data from the reproduction of the MUST field experiment in the wind tunnel "WOTAN" in the University of Hamburg were used [17, 18]. The laboratory model accurately reproduced the entire geometry of the field experiment with the scale factor 1:75. The data of this experiment are widely used for assessment of models of microscale atmospheric transport in built-up areas [18, 19].

Simulation in OpenFoam was performed for the conditions of one of the experiments, which is characterized by the undisturbed wind direction of -45° and wind speed of 8 m/s at the roof level. The measured wind profile was close to the logarithmic profile with a roughness length equal to 0.0165 m. A point source of emission with the volumetric release rate of 3.3×10^{-6} m^3/s was located at ground level be-

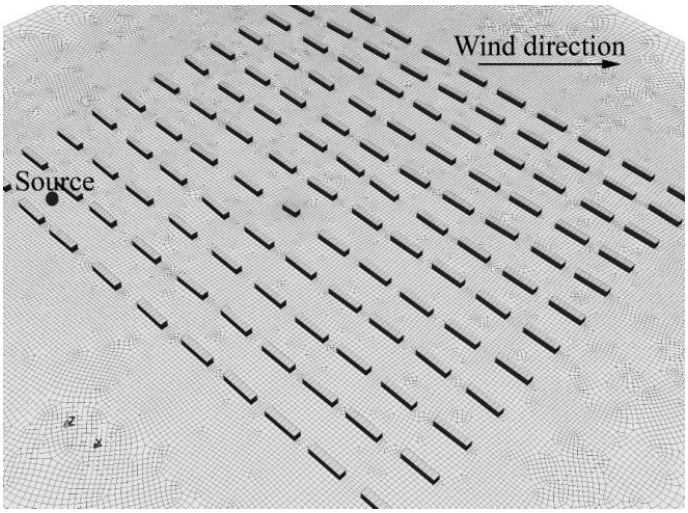

Fig. 4: Computational grid and general view of the MUST experiment.

tween the containers. An array of 256 detectors placed at 1.28 m height was used to measure the concentrations. Meteorological sensors were located at two different levels: 1.275 m and 2.55 m. The collected measurement data as reported in [18] were used in this work for comparison with the results of simulations.

Since wind tunnel reproduced turbulence and transport in the atmospheric surface layer only, the rotation effects were switched off in simulations for the conditions of this experiment ($f = 0$). In the created model of the MUST experiment for the two inlet vertical boundaries and the upper boundary wind velocity components were set according to the standard logarithmic wind profile. For the two outlet vertical boundaries through which wind blows from the computational domain, zero gradient boundary conditions were used. For the walls of the containers and bottom surface two different boundary conditions were used: aerodynamically smooth surfaces and wall functions with a small value of roughness ($z_0 = 0.001$ m). Both calculations were performed with the modified $k-\varepsilon$ turbulence model. The computational grid consisted of 36 vertical levels with a minimum horizontal dimension of about 1 m.

Figure 5 shows measured and calculated with the fixed Schmidt number (Sc $=$ 0.9) concentration fields. The use of wall functions even with the very small value of roughness made it possible to more accurately reproduce the turn of the centerline of the concentration field with respect to unperturbed wind direction as compared to the calculation with aerodynamically smooth surfaces (Fig. 5). This is confirmed by the statistical indicators – mean error (ME) and root mean squared error (RMSE) of the simulated wind speed and wind direction fields as compared to measurements (Table 1).

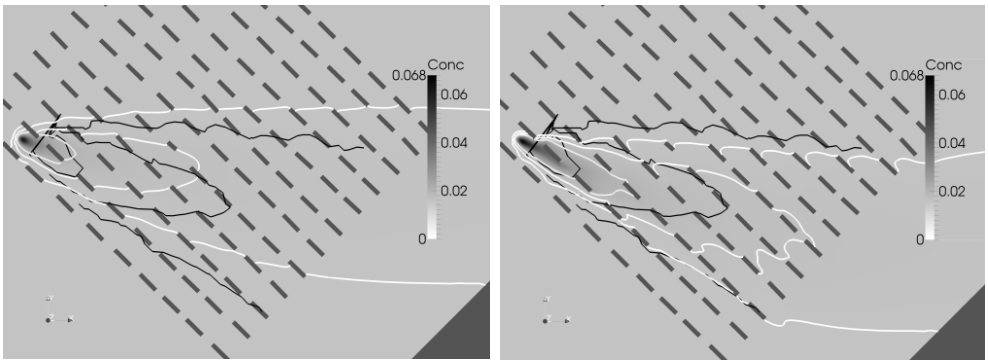

Fig. 5: Measured [18] and calculated with Sc $= 0.9$ concentration fields. Isolines are plotted for the following values of non-dimensional concentration: 0.0001, 0.001, and 0.005 (black isolines – measured values, white isolines – simulated values); solid surfaces were aerodynamically smooth (left), wall functions for solid surfaces were used (right).

Table 1: Statistical indicators of errors of simulated wind speed and wind direction as compared to measurements in MUST experiment

	$H = 1.275$ m				$H = 2.55$ m			
	WS (m/s)		WD (deg)		WS (m/s)		WD (deg)	
Boundary condition	ME	RMSE	ME	RMSE	ME	RMSE	ME	RMSE
Smooth surfaces	1.1	1.5	10.0	17.9	1.3	1.5	3.3	8.5
Wall function	0.9	1.2	-3.6	13.0	0.6	1.0	1.6	5.3

At the same time, the concentration statistics, obtained with Sc $= 0.9$, turned out to be better for calculation with aerodynamically smooth walls (Table 2). The normalized mean squared error NMSE of the simulated results as compared to measurements in the MUST experiment was NMSE $= 0.8$ for calculation with smooth

Table 2: Statistical indicators of errors in simulated concentrations as compared to measurements in the MUST experiment

	Standard Schmidt number			Optimal Schmidt number		
Boundary condition	Sc	NMSE	FB	Sc	NMSE	FB
Smooth surfaces	0.9	0.8	-0.08	1.11	0.59	-0.08
Wall function	0.9	2.6	0.4	0.43	0.61	0.03

surfaces and NMSE $= 2.6$ in calculation with the wall functions. Such discrepancy is because the accuracy of the simulated concentration distribution depends not only on the accuracy of the wind field and turbulent viscosity but also on the turbulent Schmidt number.

Therefore, the simulated results were further improved by choosing the optimal Sc values. As follows from the results in Table 2 selection of the optimal Schmidt number made it possible to obtain NMSE $= 0.6$ at a small Fractional Bias (FB) values for both types of boundary conditions on solid surfaces. The optimal values of the Schmidt number were Sc $= 1.11$ for calculation with smooth surfaces and Sc $= 0.43$ for calculation with the wall functions. Because in simulations with the wall functions better agreement with wind speed measurements was obtained as mentioned before, the estimate for the Schmidt number Sc $= 0.43$ could be considered more reliable.

4.3 Example of Model Application to Simulation of Air Pollution from the Facilities of the Former Pridneprovsky Chemical Plant

The Pridneprovsky Chemical Plant (PChP, Kamianske, Ukraine) was one of the largest uranium processing enterprises in the Soviet Union. The total amount of radioactivity (isotopes of ^{238}U, ^{234}U, ^{226}Ra, ^{210}Po, ^{230}Th) presently stored at the territories of the former PChP is estimated as 3.2×10^{15} Bq [20]. On the territory of the former PChP, there are contaminated buildings and other objects that were involved in the production technological cycle. At the same time, the industrial site of the PChP is located in about 1 km to the residential area of the city Kamianske (former Dniprodzerjinsk), and there are also operating private enterprises on the territory of the former PChP. One of the most dangerous contaminated buildings on the territory of the former PChP is Building No. 103 (48.4942 N, 34.6775 E), near which, at a distance of about 10 m from the north side, there is an operating private enterprise in Building No. 102. The risk assessment related to Building No. 103, including scenarios of routine releases from this building and releases following assumed building demolition was considered in study [21]. In previous work by Kovalets et al. [21] air pollution created by routine releases in the closest vicinity of Building No. 103 up to about 150 m was considered. The method developed in the present work allows for estimation of air pollution created by this building in the far greater region (including inhabited districts of the Kamianske city) with keeping the same resolution close to Building No. 103 as in previous work [21].

The calculations were carried out on a non-structured grid with a total horizontal size of 22×16 km^2, with the center of the computing area shifted towards the central part of Kamianske (to completely cover the territory of Kamianske). The mesh was refined in the vicinity of the PChP with the cells having the minimum horizontal size of 1 m near the contaminated building. The height of the computational do-

main was 3 km which was resolved by 63 vertical levels. The minimum vertical size of grid cells was 1 m near the ground surface. The total number of computational cells was about six million. The global SRTM 30 data set (www2.jpl.nasa.gov/srtm) was used as topography data. Modis (lpdaac.usgs.gov/products/mcd12q1v006) and Globeland-30 (www.globallandcover.com) datasets were used as underlying surface data.

Similar to previous work [21] the ventilation flux of contaminant through the windows of Building No. 103 was set proportional to the parallel and normal to the wall components of wind speed, concentration inside building Cs, and the total ventilation area with the same proportionality coefficients as in [21]. The ventilation area was set to equal to the total area of the wall for obtaining the conservative estimates. The wind profile at the entrance lateral boundaries corresponded to the results of the calculations of the "Leipzig" profile described above, but with geostrophic wind directed along the latitude of Building No. 103 towards Kamianske city. Figure 6 shows the corresponding wind field around Building No. 103 and the characteristic secondary circulation features created by the interaction of airflow with buildings. Figure 7 shows the corresponding field of concentrations normalized on concentration inside building: $c = \mathrm{C/Cs}$.

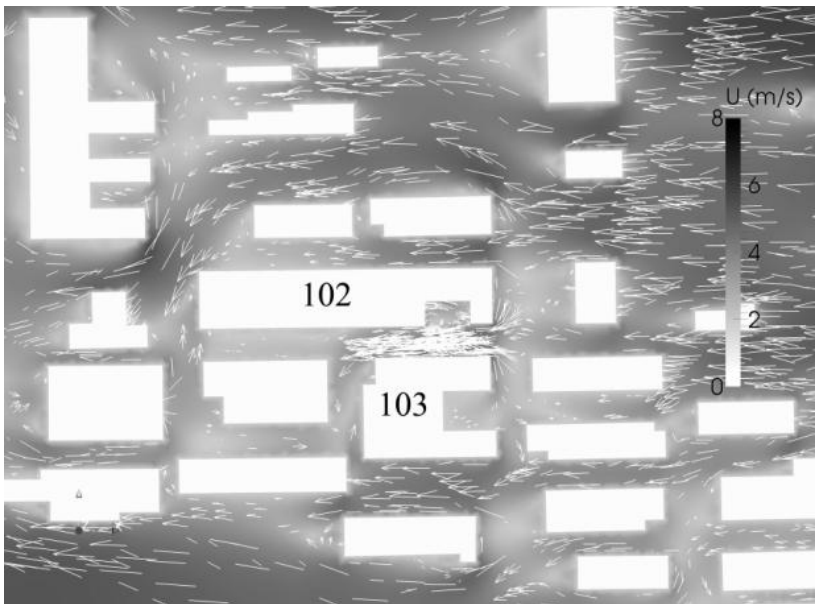

Fig. 6: Simulated wind field around the contaminated buildings of the Pridneprovsky Chemical Plant.

Fig. 7: Horizontal distribution of the normalized ground-level concentrations created by the contaminated Building No. 103 of the Pridneprovsky Chemical Plant in the area of Kamianske city (former Dniprodzerjinsk) . Isolines are plotted for the normalized concentration values: 1e-5, 1e-4, 2e-4, 1e-3, 1e-2).

The maximum value of concentration near the wall of Building No. 102 in the considered scenario reaches 1.2 due to a strong increase of concentration flux from Building No. 103 as a consequence of wind directed along the wall and increased in magnitude (Fig. 6). In the residential areas of Kamianske, the normalized concentrations reach the value of 0.01. If radon-222 is considered for which concentration inside building is known from measurements [20, 21] this value of normalized concentration corresponds to the value of volumetric concentration of radon-222 created by the Building No. 103 in residential areas of Kamianske city from 10 to 60 Bq/m^3 for this release scenario.

5 Conclusions

The hydrodynamic model of air pollutants' transport was developed based on the OpenFoam CFD code. By performing calculations on unstructured grids and using the modifications of turbulence parameterizations to account for the influence of

Earth's rotation on PBL structure, the developed model can take into account the influence of urban obstructions and complex topography on atmospheric dispersion and is suitable for estimating the spatial distribution of atmospheric pollution on a city scale ($\sim$ 10 km), while the resolution could be detailed down to the scales of individual houses and streets (˜1 m) in the areas of interest. The methodology and software tools were developed for the creation and coordinate binding of the unstructured computational grid using GMSH and the GoogleEarth software programs. In the proposed algorithm it possible to bind the unstructured grid cells resolving urban obstructions to the topography of the underlying surface. The shape and orthogonality of the upper and side surfaces of buildings as represented by the computational grid are maintained, while the lower edge of buildings follows the varying topography.

The model was successfully verified using the data of the field experiment on PBL structure ("Leipzig" profile), for which change of wind speed and wind direction with height together with height dependence of turbulent viscosity was successfully reproduced. Applicability of the model on a micro-scale was tested by application for the conditions of the MUST experiment on atmospheric transport in the array of cubical obstacles. The obtained statistical characteristics of errors of calculated results as compared to measurements in the MUST experiment (NMSE ≈ 0.6) are comparable with the results of other known models as presented in [18]. The optimal Schmidt number with which the best accuracy of the calculated results was achieved for the MUST experiment was sensitive to the used parameterizations of boundary conditions. The parameterization of bottom boundary conditions which used wall functions with small roughness value provided the best accuracy of the calculated wind fields as compared to measurements. The corresponding optimal value of Sc ≈ 0.4 was obtained for this parameterization.

The applicability of the developed model for the solution of the practical problems was demonstrated by the example of the assessment of atmospheric pollution in the vicinity of the highly contaminated Building No. 103 located on the territory of the former uranium production facility Prindeprovsky Chemical Plant (Kamianske, Ukraine). In contrast to previous works that considered the nearest vicinity of this building, the developed approach allowed for estimation of the possible levels of contamination that could be created by the routine releases from the Building No. 103 for the whole Kamianske city with preserving fine resolution in the areas of special interest. In the nearest residential areas of Kamianske concentrations of radon-222, created by the contaminated building, could reach the values up to 60 Bq/m^3 in the conservative release scenario. The developed model could be especially useful for safety assessments in the vicinities of similar hazardous facilities, which, on the one side, require detailed analysis of the pollutants' distribution around specific areas of

interest and, on the other side, require an assessment of air pollution in a relatively large region.

ACKNOWLEDGEMENTS

This work was supported by the Grant of the National Research Foundation of Ukraine No. 2020.02/0048 (I. Kovalets) and by funding from the National Academy of Sciences of Ukraine, project No. 0119U001433 (A. Khalchenkov).

REFERENCES

[1] M. LATEB, R.N. MERONEY, M. YATAGHENE, H. FELLOUAH, F. SALEH, M.C. BOUFADEL (2016) On the use of numerical modelling for near-field pollutant dispersion in urban environments – A review. *Environmental Pollution* **208** 271-283.

[2] C. LI, Y. XU, M. LIU, Y. HU, N. HUANG, W. WU (2020) Modeling the Impact of Urban Three-Dimensional Expansion on Atmospheric Environmental Conditions in an Old Industrial District: A Case Study in Shenyang, China. *Polish Journal of Environmental Studies* **29**(5) 3171-3181.

[3] Z. GAO, R. BRESSON, Y. QU, M. MILLIEZ, C. DE MUNCK, B. CARISSIMO (2018) High resolution unsteady RANS simulation of wind, thermal effects and pollution dispersion for studying urban renewal scenarios in a neighborhood of Toulouse. *Urban Climate* **23** 114-130.

[4] K. SYNYLO, O. ZAPOROZHETS, J. STILLER, J. FRHLICH (2017) Improvement of airport local air quality modeling. *Journal of Aircraft* **54**(5) 1750-1759.

[5] OpenCFD Limited (accessed March 12, 2021) OpenFOAM: The Open Source CFD Toolbox, User Guide Version v2012. https://deac-riga.dl.sourceforge.net/project/openfoam/v2012/UserGuide.pdf.

[6] A.E. CHATZIMICHAILIDIS, C.D. ARGYROPOULOS, M.J. ASSAEL, K.E. KAKOSIMOS (2019) Qualitative and Quantitative Investigation of Multiple Large Eddy Simulation Aspects for Pollutant Dispersion in Street Canyons Using OpenFOAM. *Atmosphere* **10**(1) 17.

[7] A.S. MONIN, A.M. YAGLOM (1971) "Statistical fluid mechanics: Mechanics of turbulence". Volume 1. MIT Press, Cambridge, UK.

[8] J.R. GARRATT (1998) "The atmospheric boundary layer". Cambridge University Press, Cambridge, UK.

[9] W.P. JONES (1980) Models of the turbulent flows with variable density and combustion, In: W. Kollmann (ed.) "Prediction methods for turbulent flows", Hemisphere Pub.,Washington DC., pp. 349-398.

[10] A.K. BLACKADAR (1962) The vertical distribution of wind and turbulent exchange in a neutral atmosphere. *Journal of Geophysical Research* **67**(8) 3095-3102.

[11] D.D. APSLEY, I.P. CASTRO (1997) A limited-length-scale $k-\varepsilon$ model for the neutral and stably-stratified atmospheric boundary layer. *Boundary-Layer Meteorology* **83**(1) 75-98.

[12] F. XUE, X. LI, R. OOKA, H. KIKUMOTO, W. ZHANG (2017) Turbulent Schmidt number for source term estimation using Bayesian inference. *Building and Environment* **125** 414-422.

[13] C. GEUZAINE, J.F. REMACLE (2009) GMSH a three-dimensional finite element mesh generator with built in pre and post processing facilities. *Journal for Numerical Methods in Engineering* **79**(71) 1309-1331.

[14] O.V. KHALCHENKOV (2017) Preparation of a computational finite-volume unstructured grid for three-dimensional CFD modeling of the surface layer of the atmosphere in the urban area using the OpenFoam software package. *Mathematical Machines and Systems* N2 110-119. (in Russian)

[15] H.H. LETTAU (1962) Theoretical wind spirals in the boundary layer of a barotropic atmosphere. *Beiträge zur Physik der Atmosphäre* **35** 195-212.

[16] H.W. Detering, D. Etling (1985) Application of the E-ε turbulence model to the atmospheric boundary layer. *Boundary-Layer Meteorology* **33** 113-133.

[17] B. LEITL, K. BEZPALCOVA, F. HARMS (2007) Wind tunnel modelling of the MUST experiment. In: Proceedings of the 11th Int. Conf. on Harmonisation within Atmospheric Dispersion Modelling for Regulatory Purposes (HARMO 2007). Cambridge, UK, 2-5 July, 2007.

[18] M. SCHATZMANN, H. OLESEN, J. FRANKE (accessed March 12, 2021) COST 732 Model Evaluation Case Studies: Approach and Results. https://mi-pub.cen.uni-hamburg.de/fileadmin/files/forschung/techmet/cost/cost_732/pdf/5th_Docu_May_10.pdf.

[19] G.C. EFTHIMIOU (2019) Prediction of four concentration moments of an airborne material released from a point source in an urban environment. *Journal of Wind Engineering and Industrial Aerodynamics* **184** 247-255.

[20] T. LAVROVA, O. VOITSEKHOVYCH (2013). Radioecological assessment and remediationplanning at the former uranium milling facilities at the Pridnieprovsky Chemical Plant in Ukraine. *J. of Environmental Radioactivity* **115** 118-123.

[21] I. KOVALETS, A. KCHALCHENKOV, T. LAVROVA (2013) Modelling of the atmospheric dispersion of radionuclides from the uranium processing facilities of the former Pridneprovsky Chemical Plant in Ukraine. In: R. San Jose, J.L. Perez (eds) "Proceedings of the 15th Int. Conf. on Harmonisation within Atmospheric Dispersion Modelling for Regulatory Purposes, HARMO 2013", Environmental Software and Modelling Group, Madrid, pp. 618-622.